

Original Article

Transcriptomic analysis of dracorhodin perchlorate intervention in wound healing in SD rats

Xiao-Wen Jiang*, Xu Guo*, Yao Wang, Yuwen Han, Wenhui Yu

Department of Veterinary Medicine, Northeast Agricultural University, 59 Mucai Street, Xiangfang District, Harbin, China. *Equal contributors.

Received November 12, 2018; Accepted April 10, 2019; Epub August 15, 2019; Published August 30, 2019

Abstract: A rat model of skin wounding was used to examine the effects of Dracorhodin perchlorate (DP) on regulation of genes related to wound healing. Samples were taken on day 8 after wound formation. Transcriptomics analysis was performed using second-generation sequencing techniques. Regulation of genes related to wound healing under DP intervention was also subjected to bioinformatics analysis. Results: A total of 243 genes were upregulated and 538 genes were downregulated in the DP group. GO analysis revealed that upregulated and downregulated genes in the DP group were associated with 1,220 and 1,267 GO enrichment terms, respectively. KEGG analysis showed that upregulated and downregulated genes were enriched in 189 and 223 pathways, respectively. Upregulated genes were mainly enriched in cGMP-PKG signaling pathways. Conclusion: Wounding-related genes in the DP test group and Vaseline control group were screened separately. Screening revealed that 243 and 538 genes in the DP group were upregulated and downregulated, respectively. Results of GO and KEGG enrichment analysis suggest that DP can inhibit inflammation and accelerate biological activities related to wound healing

Keywords: Dracorhodin perchlorate, wound healing, transcriptomics, GO, KEGG

Introduction

Wound healing is the repair of damaged skin tissue. This process includes three stages, inflammatory reaction, healing, and remodeling [1, 2]. Various types of cells, such as keratinocytes and fibroblasts, participate in this biological process. Wound healing also involves migration, proliferation, differentiation, microbubble release, and various other cellular activities [3, 4]. It includes a large number of biological factors, such as TGF, EGF, and FGF, as well as diverse regulatory pathways, such as WNT and ERK pathways [5-8]. Long-chain noncoding (lnc) RNAs play an important role in this process [9]. A high-throughput gene sequencing experimental method is needed, enabling the simultaneous study of the maximum number of molecules. This will allow researchers to grasp various changes exhibited by tissues during wound healing. This approach will aid in understanding the regulation of wound repair and reveal the relationship between gene expres-

sion and wound repair. Omics technology can meet the above requirements. Current second-generation sequencing technology is characterized by high throughput, high accuracy, and facile operation [10]. It has been widely used by researchers [11] in microbiology and other aspects of research [12].

Dragon's blood is a red resin produced by the palm plant. It has been extensively used in the traditional medicine of various nations. It has a wide variety of pharmacological functions, including hemostatic, anti-inflammatory, and antioxidative functions [13]. It also exerts protective effects against brain damage [14]. Dracorhodin perchlorate (DP) is a stable form of hemoglobin extracted from the blood, commonly used to treat skin wounds [15, 16]. DP promotes fibroblast proliferation, collagen formation, and epithelial and vascular regeneration. It accelerates wound healing [17, 18] and intervenes in scar formation [19]. Many other studies have suggested that it has the ability to pro-

mote apoptosis [20-22] and fight against multiple cancers, including lung cancer and breast cancer [23, 24]. To further reveal the molecular mechanisms of DP in promoting wound repair, this experiment examined its regulation characteristics in wound repair using transcriptomics. The aim of the current study was to provide scientific basis for the application of blood in wound treatment.

Methods and materials

Experimental reagents and instruments

Main instruments used in this study were as follows: NanoDrop 2000 Thermo Fisher Scientific, USA; Invitrogen Qubit 3.0 Spectrophotometer Thermo Fisher Scientific, USA; ABI 2720 Thermal Cycler Thermo Fisher Scientific, USA; Eppendorf 5810R Centrifuge Eppendorf, Germany; Agilent 2100 bioanalyzer Agilent Technologies, USA; Illumina cbot Cluster Station Illumina, USA; Illumina HiSeq 2500 Illumina, USA; and Ambion Magnetic Stand Thermo Fisher Scientific, USA.

Main reagents utilized in this work were as follows: TruSeq Stranded Total RNA Library Prep Kit Illumina, USA; SuperScript IV Reverse Transcriptase Thermo Fisher Scientific, USA; Agencourt SPRiSelect Reagent Kit Beckman Coulter, USA; TruSeq smallRNA sample Preparation kit Illumina, USA; T4 RNA Ligase 2, truncated NEB, UK; Corning® Costar® Spin-X® centrifuge tube; Filters, Sigma-Aldrich, USA; Agilent High Sensitivity DNA Kit Agilent Technologies, USA; Novex® TBE Running Buffer (5X) Thermo Fisher Scientific, USA; Acrylamide/Bis 19:1, 40% Thermo Fisher Scientific, USA; Novex® Hi-Density TBE Sample Buffer (5X) Thermo Fisher Scientific, USA; DP (≥99%; Pharmaceutical Inspection Institute, Harbin, China); Vaseline, China; Chloral hydrate, China.

Methods

Preparation and grouping of rat skin injury models: Nine healthy Sprague-Dawley (SD) rats were purchased from Changchun Yisi Experimental Animal Company. All rats were male and weighed approximately 180-220 g. Model construction was initiated after 1 week of conventional adaptive feeding. They were randomly allocated into the drug-administered group, Vaseline control group, and blank group. Each group included three rats. Skin defects, with

diameters of approximately 10 mm, were created using a sterilized puncher. The drug-administered group was treated with DP ointment, while the control group was treated with Vaseline ointment for 7 days. Animals were treated in accordance with the provisions of the Guiding Opinions on Treating Experimental Animals issued by the Ministry of Science and Technology of the People's Republic of China.

Extraction of mRNA: The rats were quickly sacrificed on the eighth day of the experiment. Skin tissues around each wound were cut with a pair of sterilized scissors. They were washed with sterilized PBS solution, frozen in liquid nitrogen, and finally frozen in dry ice. They were sent to Genesky Biotechnologies Inc., Shanghai, for testing.

Removal of rRNA and purification and fragmentation of RNA: An appropriate amount of total RNA was collected for rRNA removal. Total RNA was incubated with species-specific rRNA (human/mouse/rat). Moreover, rRNA was captured using probes modified with biotin and magnetic beads coated with streptavidin. Probes were bound to the rRNA complexes for rRNA removal. After another round of AMPure XP magnetic bead purification, RNA contaminants, including mRNA with and without polyA, noncoding RNA, and regulatory RNA, were removed from the rRNA sample. A buffer consisting of eluted, fragmented, and random primers was added to the sample. Next, fragmentation was performed during the completion of random primer binding in the next stage of cDNA synthesis. The product was incubated at a high temperature of 94°C for thermal cleavage. The fragments had lengths of 100-300 bp. This range is highly suitable for the 2 × 150 bp sequencing mode. The duration of fragmentation was optimized based on the integrity of the original RNA.

Reverse transcription of first-strand cDNA: First-strand cDNA was synthesized through the fragmented short fragment RNA, in the presence of one-chain synthesis buffer and Invitrogen reverse transcriptase SuperScript IV. It was applied as a template after binding a random reverse transcription primer. Actinomycin D was added to the solution to prevent false reverse transcription. The specificity of reverse transcription was ensured, using RNA as a template.

Transcriptomic of wound healing

Synthesis of second-strand cDNA: The two-stranded synthetic premix system was added to the system for first-strand cDNA synthesis. In this reaction, RNA on the RNA/cDNA hybrid strand was first hydrolyzed. Afterward, the DNA polymerase used the one-strand cDNA as a template. A dNTP mix containing dTTP was used replaced with dUTP as a substrate to synthesize for the synthesis of double-stranded cDNA with dUTP. Given the subsequent PCR amplification step, the high-fidelity polymerase cannot recognize and amplify the second-strand cDNA that had been randomly incorporated with dUTP. Thus, only one strand was amplified. Library information of the strand cDNA was used to construct the strand-specific library. After purification with Agencourt AMPure XP magnetic beads, double-stranded cDNA (Double-strand cDNA, ds cDNA) with "A" directly at both ends was obtained.

Screening of the fragment library: The cDNA library was created. The Agencourt SPRIselect nucleic acid fragment screening kit was used to perform fragment screening, simultaneously with library purification. Using double size selection, SPRI beads were used to remove the left-side size selector. The right-side size selector was also removed. The original library, with a fragment peak at 300 bp, was used for the next PCR amplification. After library purification, excess sequencing linkers in the system and the self-ligated product of the linker were removed, preventing inefficient PCR amplification and eliminating influences on machine sequencing.

PCR amplification of the cDNA library: High-fidelity polymerase was used to amplify the original library in a 50 μ L reaction system. This was to ensure an ample total library size for the upper sequencer. Only DNA fragments with a linker at both ends were amplified. Fragments that were only ligated to the single-ended linker were removed. The qualified library was enriched. The high-fidelity polymerase was blocked given the presence of the dUTP on the new double-stranded cDNA. Amplification of this template allowed the amplified library to be derived only from one-strand cDNA. Chain direction information was faithfully retained. The number of PCR amplification cycles ranged from 12-15. Deviation introduced by the excessive number of amplification cycles was reduced, ensuring ample amounts of product.

The amplified library was purified with magnetic beads, obtaining a sequencing library that could be used for machine sequencing.

Quality testing and quantification of the sequencing library: The constructed sequencing library was subjected to quality checking and quantification. Library concentrations were accurately quantified using Qubit and the library fragment size distribution was determined by using an Agilent 2100 Bioanalyzer, assessing its suitability for machine sequencing. Qualified samples were diluted in accordance with sequencing requirements. Multiple samples were mixed on the machine in accordance with the corresponding ratio (molar ratio). The library was sequenced using an Illumina high-throughput sequencing platform with a 2 \times 150 bp double-ended sequencing strategy.

Data analysis

Data analysis mainly included biological information, total RNA quality control, raw sequencing data preprocessing, data quality filtering, reference sequence comparison analysis, mRNA standard information analysis, mRNA expression quantification, mRNA differential expression analysis, and differential gene GO and KEGG enrichment analysis. It also included variable shear analysis, new transcript prediction, fusion gene analysis, lncRNA standard information analysis, lncRNA expression quantification, lncRNA differential expression analysis, differential lncRNA GO target gene and KEGG enrichment analysis, and differential lncRNA target gene prediction.

Differentially-expressed genes between groups were analyzed using Cuffdiff software [25]. Cuffdiff assumes that the level of transcript expression under each condition can be measured based on the number of the fragments produced. Thus, changes in expression levels were measured by comparing the fragment counts under each condition. Genes are considered as differentially expressed when $P < 0.05$ and $|\log_2(\text{fold change})| > 1$, while $\log_2(\text{fold change}) > 1$ is defined as an upregulated gene (up) and $\log_2(\text{fold change}) < -1$ is defined as a downregulated gene (down).

GO and KEGG enrichment analyses were performed using the R package cluster Profiler (<http://bioconductor.org/packages/release/bioc/html/clusterProfiler.html>) [26]. These en-

Transcriptomic of wound healing

Table 1. Number of differentially-expressed RNA

	Differential mRNA		Differential LncRNA	
	DP group	Vaseline group	DP group	Vaseline group
Up-regulated genes	243	461	303	285
Down-regulated genes	538	474	328	340
Total differential genes	781	935	601	625

richment methods involved the use of the entire transcript as a background list. The candidate list of differentially-expressed genes/transcripts was selected from the background list. Hypergeometric distribution testing was applied to calculate whether the representative GO or KEGG set was enriched in the differentially-expressed gene/transcript list. *P*-values were obtained and then corrected with Benjamini and Hochberg multiple tests, obtaining the FDR.

Results

Differential gene screening

Differentially-expressed genes were screened by using Cuffdiff software with two criteria. The number of downregulated genes in each group was higher than that of upregulated genes. The number of downregulated genes in the DP group was considerably higher than that in the blank group. Screening revealed that DP and Vaseline groups shared 62 downregulated genes, such as *Adamts19* and *Adh1*. A total of 538 and 474 genes were downregulated in DP and Vaseline groups, respectively. DP and Vaseline groups shared 19 upregulated genes, such as *Bin2a*, *Brms1*, and *Chid1*. A total of 243 and 461 genes were upregulated in DP and Vaseline groups, respectively. Differential expression analysis revealed that 303 and 285 lncRNA target genes were upregulated in DP and Vaseline groups, respectively. A total of 328 and 340 lncRNA genes were downregulated in DP and Vaseline groups, respectively (**Table 1**).

GO analysis of differentially-expressed genes

Of the 781 differentially expressed genes in the DP group, 1,803 enriched GO items were selected. The majority, or 1,469, of the GO terms were allocated to the BP category, while 150 items were classified into the CC category. A total of 184 GO cell items were classified into

the MF category. The Vaseline group included 912 statistically significant GO classification items, of which 727, 81, and 105 were allocated to BP, CC, and MF classes, respectively. GO enrichment analysis was

performed, separately, for differentially upregulated and downregulated genes in DP and Vaseline groups, respectively. Moreover, 1,220 and 1,267 GO items were found for the 243 upregulated and 538 downregulated genes in the DP group, respectively. A total of 999 and 1,226 GO items were found for upregulated and downregulated genes in the Vaseline group, respectively. GO classification items with the most statistically significant top 10 enrichment levels (i.e., the highest *p*-value) in each category are shown in **Figures 1-6**.

KEGG analysis of differentially-expressed genes

Upregulated and downregulated genes with statistically significant different expression levels in the DP group were subjected to KEGG analysis. Upregulated and downregulated genes were enriched in 189 and 223 pathways, respectively. Upregulated genes showed the highest degree of enrichment in cGMP-PKG, cardiomyocyte adrenergic, and cAMP signaling pathways. Downregulated genes showed the highest degree of enrichment in systemic lupus erythematosus, alcoholism, and ribosome pathways. Comparative KEGG analysis results for the Vaseline and control groups revealed the three most prominent KEGG pathways for differential gene enrichment, including the hedgehog signaling pathway, malaria, and basal cell carcinoma. Comparing the results for the Vaseline group with those for the control group, upregulated genes exhibited the highest degree of enrichment in the estrogen signaling pathway, Hippo signaling pathway, and Cushing syndrome, whereas downregulated genes were enriched in the myocardial adrenergic signal transduction, hypertrophy cardiomyopathy, and calcium signaling pathways. KEGG scatter plots are shown in **Figures 7, 8**.

Figure 7 shows KEGG analysis results for differentially-expressed genes between DP and blank groups.

Transcriptomic of wound healing

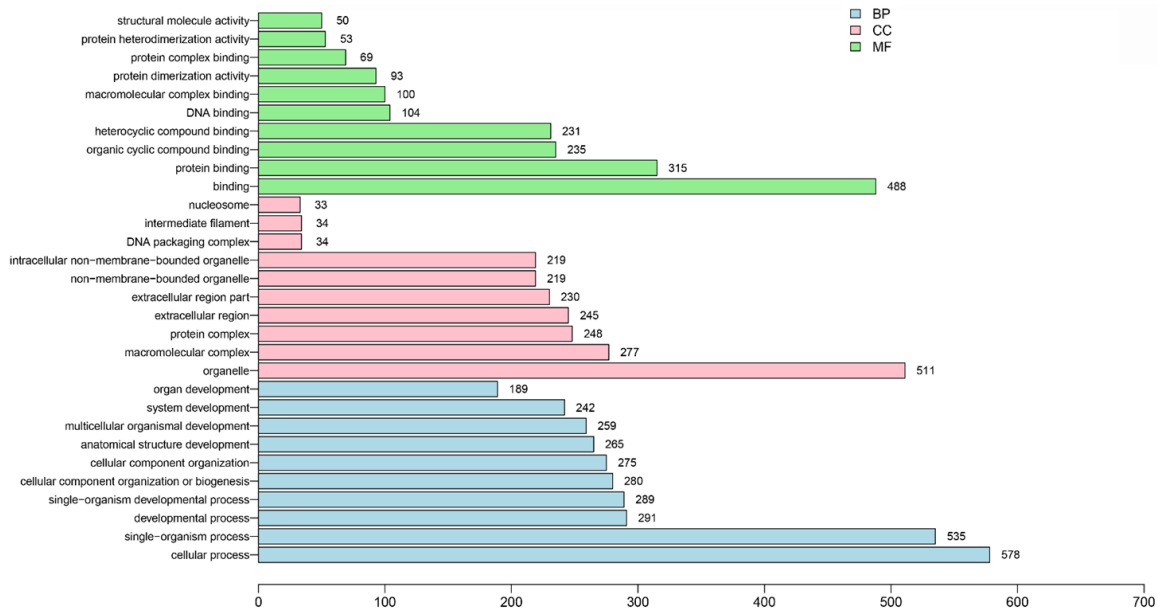


Figure 1. GO analysis results for differentially-expressed genes between DP and blank groups.

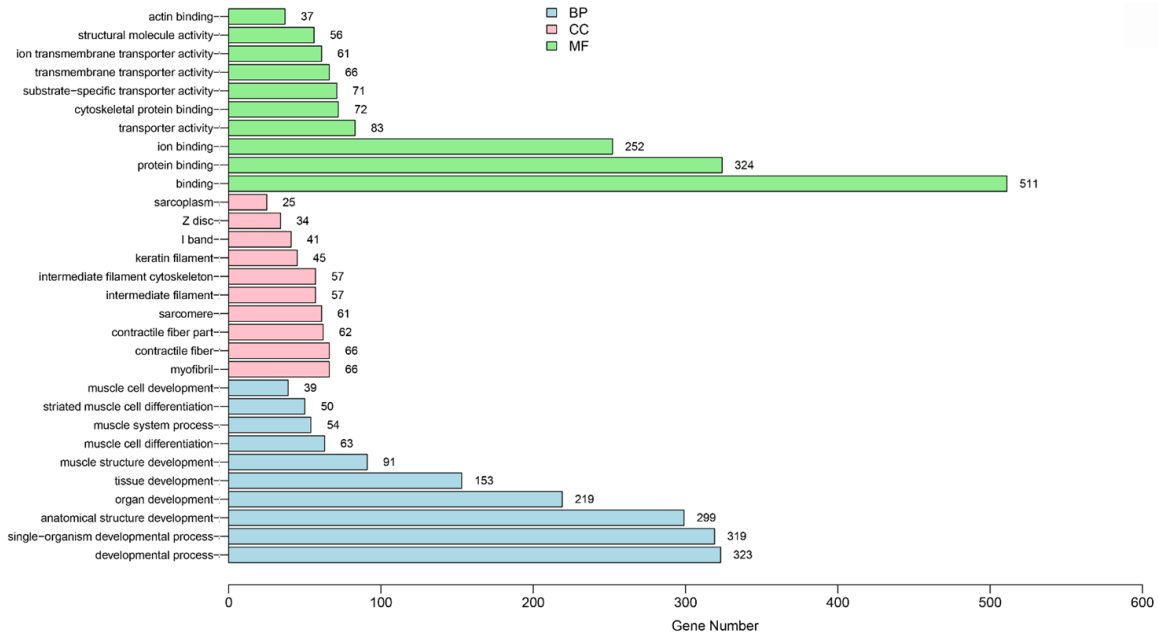


Figure 2. GO analysis results for differentially-expressed genes between Vaseline and blank groups.

GO analysis of differentially-expressed lncRNA target genes

Comparing lncRNA genes that were differentially-expressed between the DP group and blank group yielded 637 GO terms with statistical significance. Of these genes, 500, 73, and 64 items belonged to BP, CC, and MF, respectively.

Comparing lncRNA sequences between the DP and Vaseline groups yielded 612 GO terms with statistical significance, of which 460, 68, and 84 items belonged to the BP, CC, and MF categories, respectively. The term “systems development” was included in the top 10 enriched BP categories. The top 10 GO classification items in the CC categories includ-

Transcriptomic of wound healing

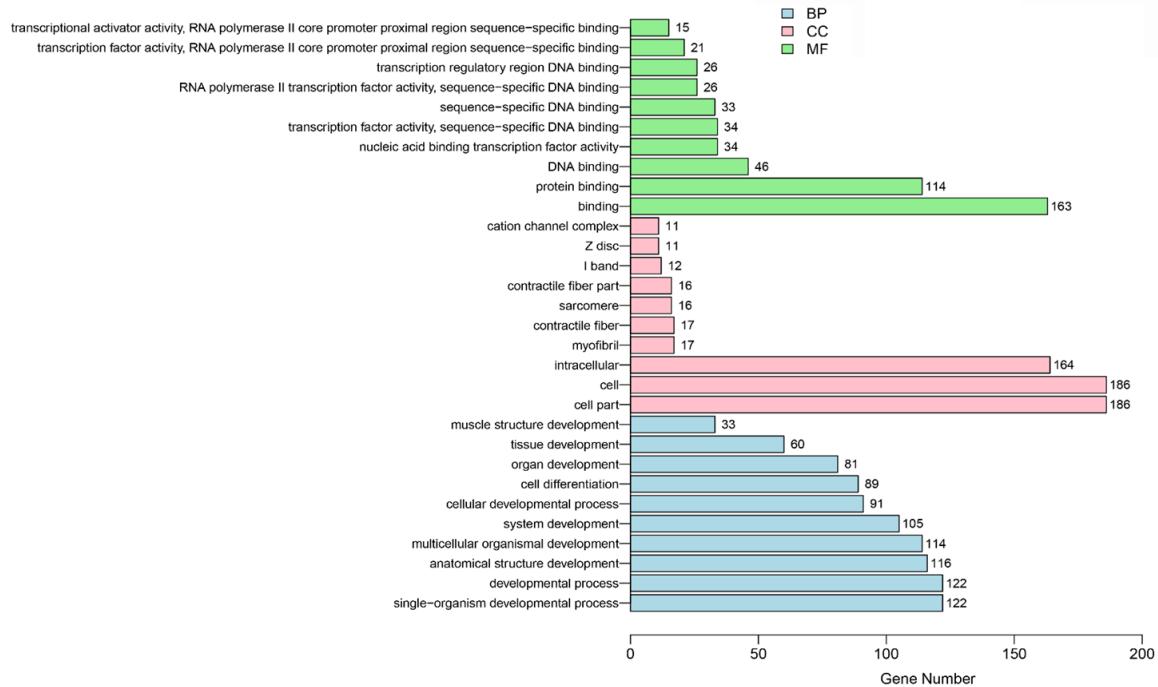


Figure 3. GO analysis results for upregulated genes between DP and blank groups.

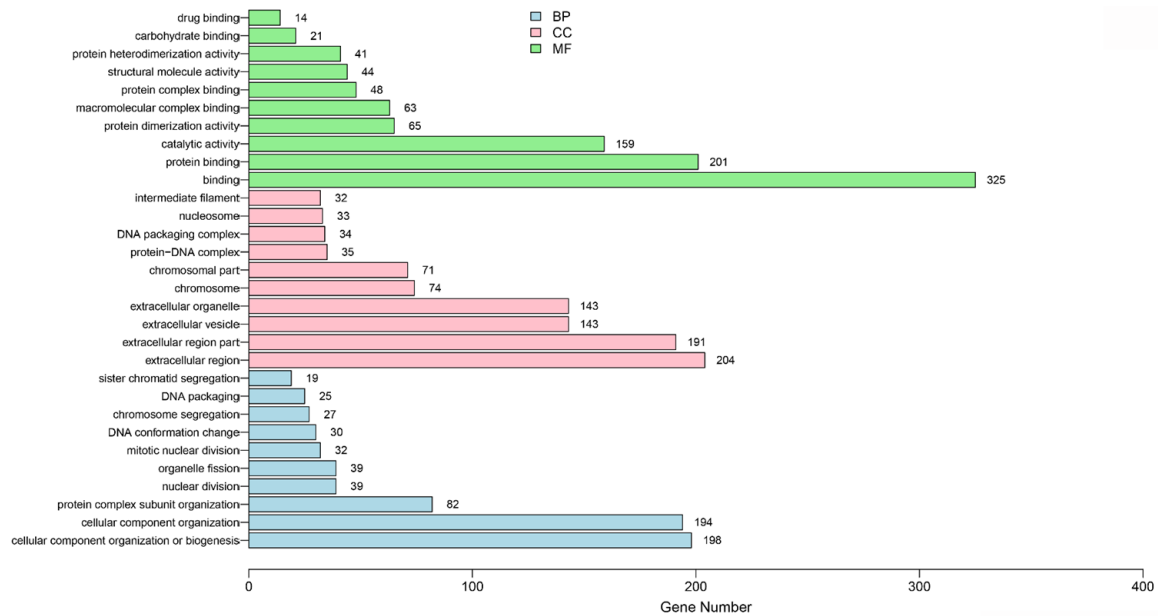


Figure 4. GO analysis results for downregulated genes between DP and blank groups.

ed the term “intracellular”. “Binding” was included in the top 10 GO classification items in the MF category. The TOP10 classification items for each category and the number of genes that they contain are shown in **Figures 9, 10**.

KEGG analysis results for target genes of differentially-expressed lncRNAs

Target genes of differentially-expressed lncRNAs between DP and control groups were enriched in 88 pathways. The three pathways with

Transcriptomic of wound healing

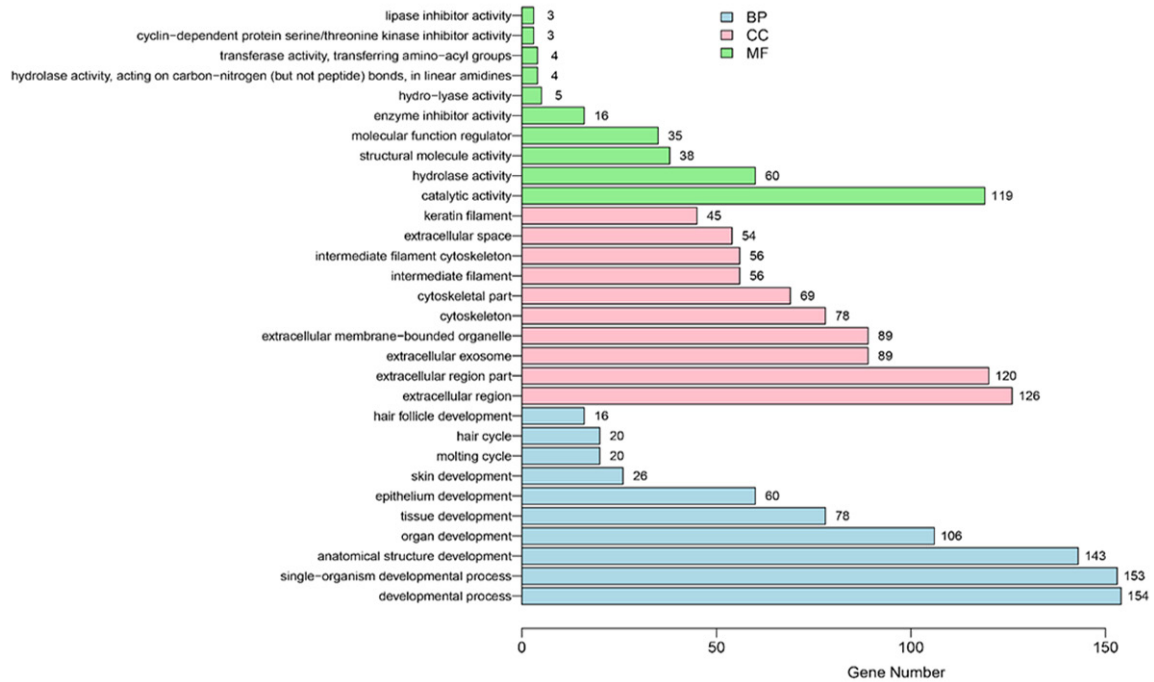


Figure 5. GO analysis results for upregulated genes between Vaseline and blank groups.

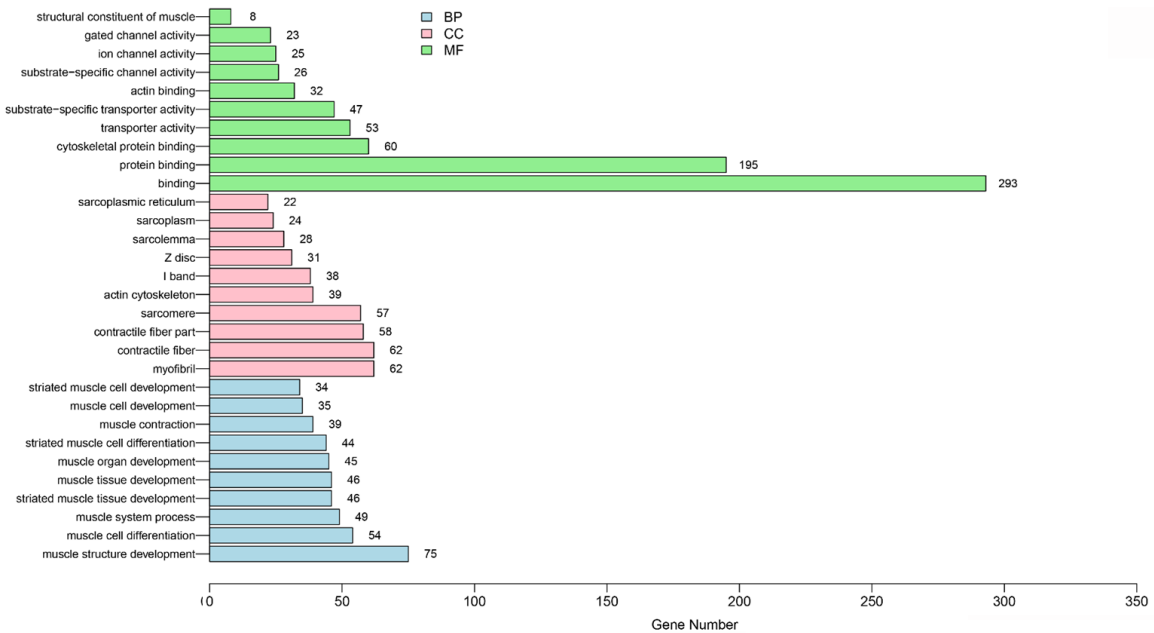


Figure 6. GO analysis results for downregulated genes between Vaseline and blank groups.

the highest enrichment were phenylalanine, bi-synthesis of tyrosine and tryptophan biosynthesis pathways, arginine and proline metabolism pathways, and bacterial invasion of epithelial cells pathway.

A total of 96 pathways were identified in Vaseline and control groups. Aldosterone-mediated sodium reabsorption, nucleotide excision repair, and endometrial cancer pathways had the highest degree of enrichment.

Transcriptomic of wound healing

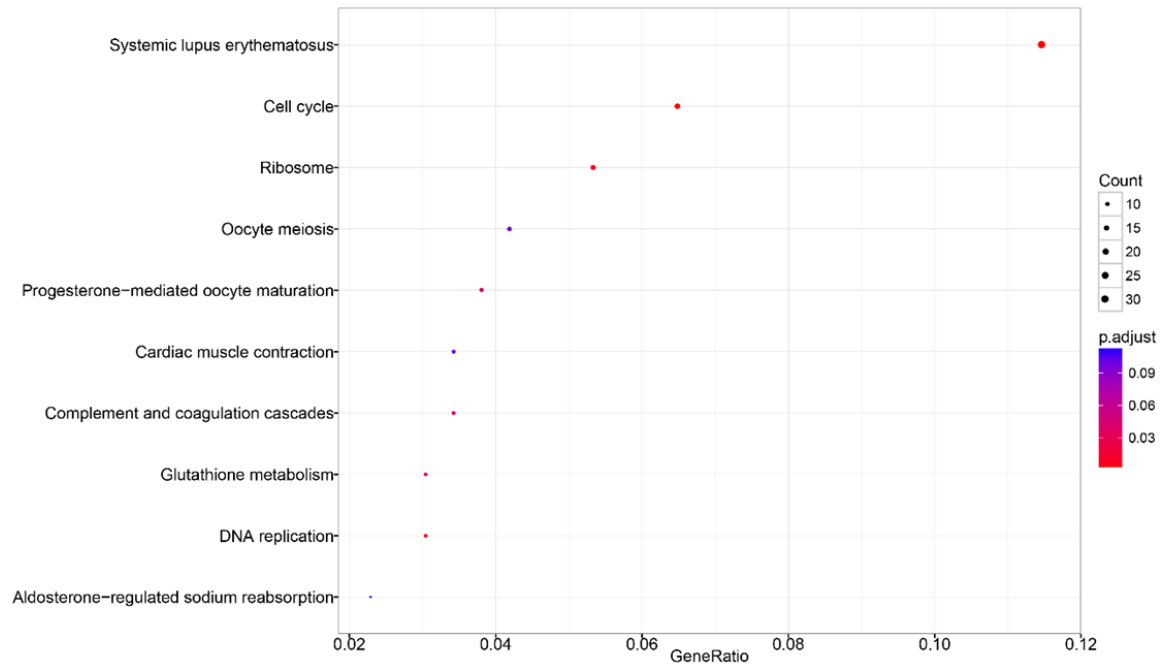


Figure 7. KEGG analysis results for differentially-expressed genes between DP and blank groups.

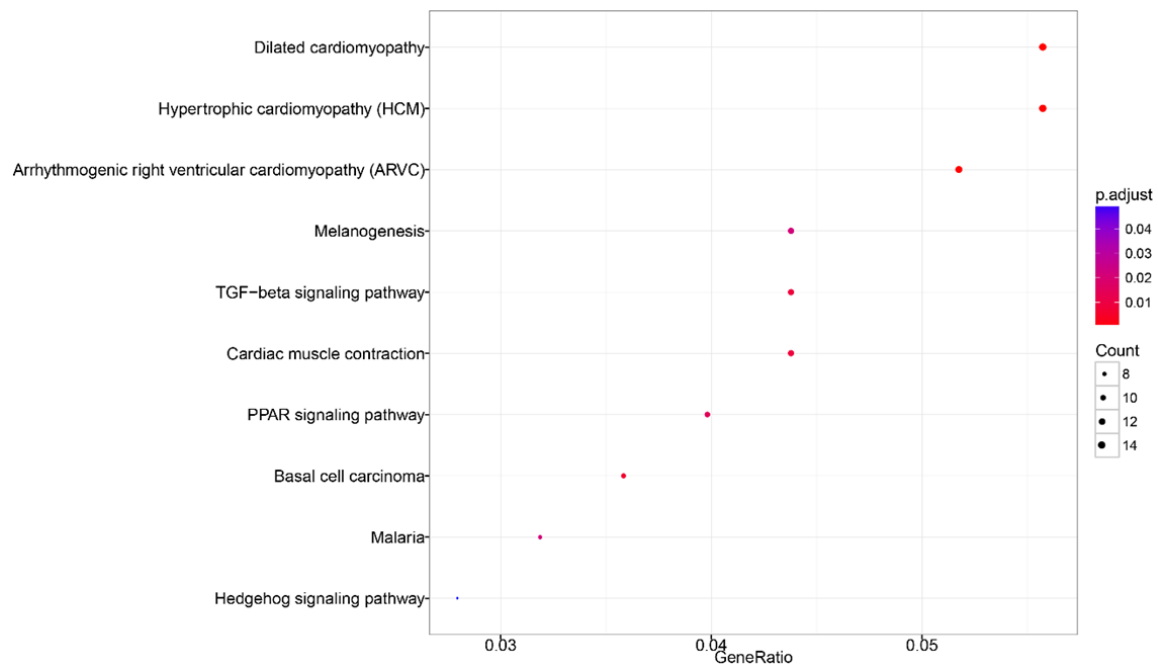


Figure 8. KEGG analysis results for differentially-expressed genes between Vaseline and blank groups.

Scatter plots of the KEGG pathways for prediction of lncRNA target genes are shown in **Figures 11, 12**.

Discussion

The number of downregulated genes in the DP group was higher than that of upregulated

genes. This result indicates that downregulated genes in the DP group may play an important role in injury development. GO enrichment analysis focused on changes in differentially-expressed genes that were categorized in BP during wound healing, given that wounding mainly involves changes in physical or biochemical processes. Functions of differential-

Transcriptomic of wound healing

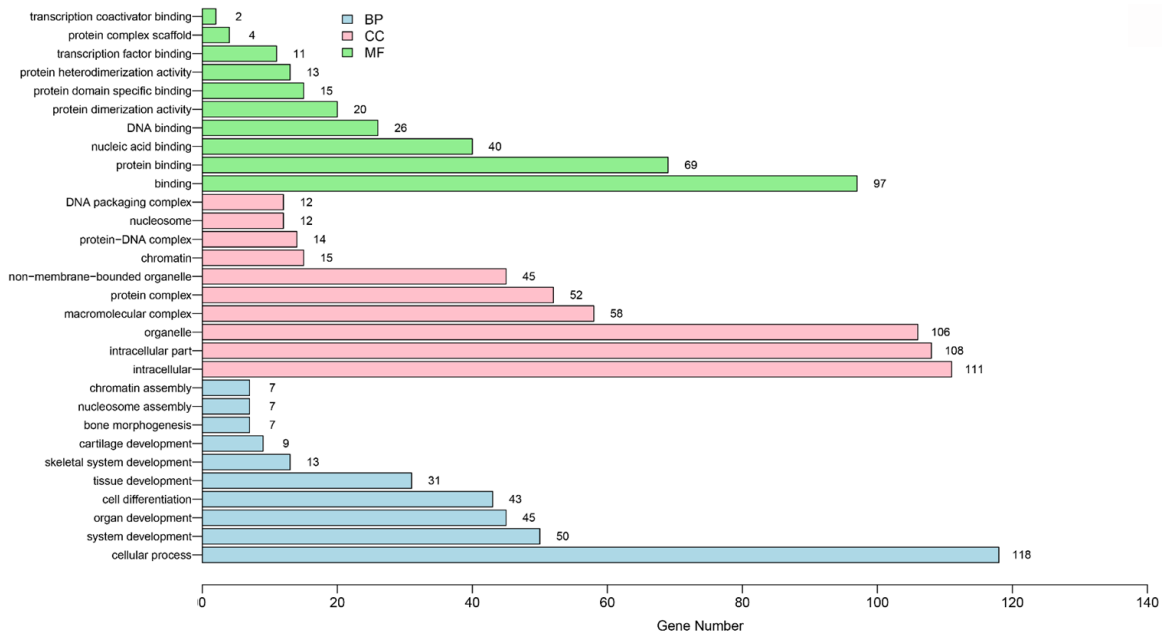


Figure 9. GO analysis results for target genes of lncRNAs with differential expression between DP and blank groups.

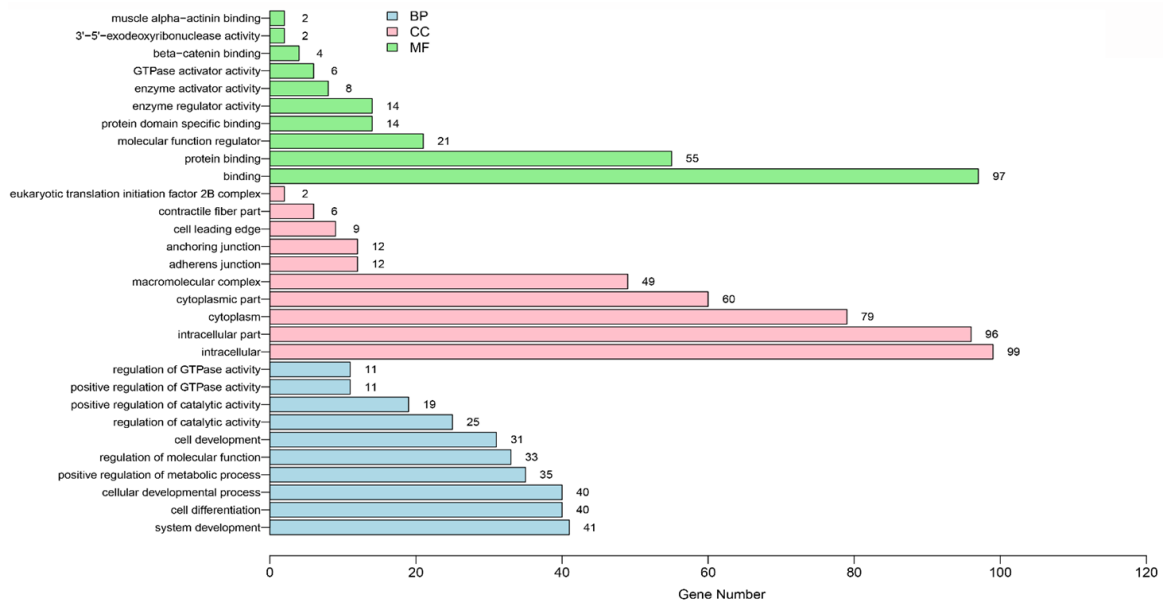


Figure 10. GO analysis results for target genes of lncRNAs with differential expression between Vaseline and blank groups.

ly-expressed genes in the DP group were mainly classified into GO:0032502 developmental process and GO:0071840 cellular component organization or biogenesis, wherein GO:0071840 in GO:0016043 cellular component organization is the main function of the genes. Differential expression of the identified func-

tional genes represents a change in tissue development. U-regulated genes mainly concentrated in GO:0032502 developmental process, GO:0044699 single-organism process, GO:0032501 multicellular organismal process, and other functions, among which GO:0032502 developmental process is the most enriched

Transcriptomic of wound healing

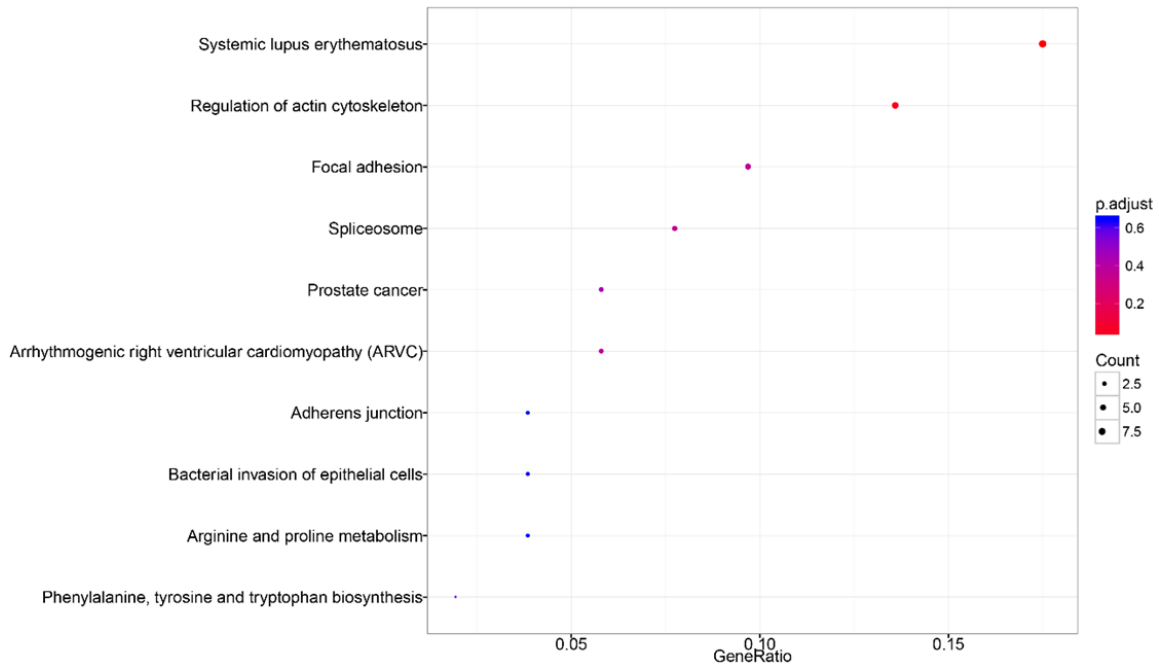


Figure 11. KEGG analysis results for predicted target genes of lncRNAs with differential expression between the DP and blank groups.

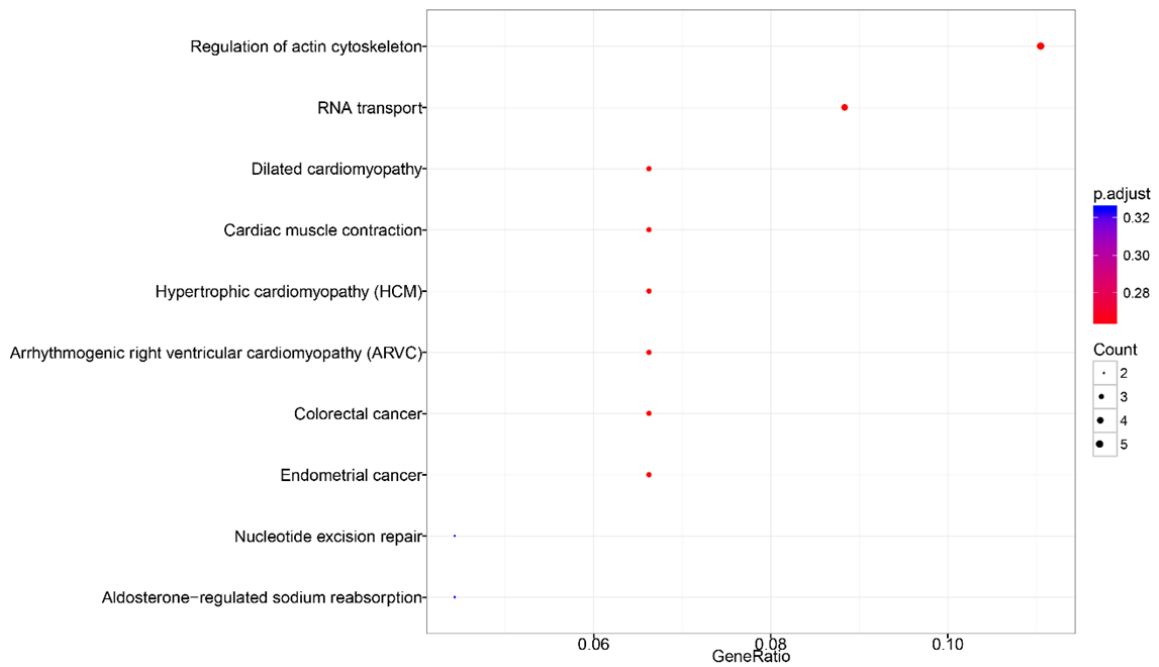


Figure 12. KEGG analysis results for predicted target genes of lncRNAs with differential expressions between Vaseline and blank groups.

and dominant. Differentially-expressed genes were also enriched in GO:0044767 single-organism developmental process and GO:0048856 anatomical structure development.

These functions are closely related to cell growth and tissue development. They are consistent with the physiological phase of wound healing and reconstruction after 7 days of

wound establishment. Downregulated genes were mainly enriched in GO:0071840 cellular component organization or biogenesis and GO:0009987 cellular process. The inclusion of GO:0016043 cellular component organization in GO:0071840 indicates that differentially-expressed genes have different functions. Notably, most of the functions of downregulated genes in the DP group are related to cell development and development. Most of the functions of the upregulated genes in the DP group are based on the development of cells on high levels, such as tissues, muscle structures, and organs. This result may be attributed to the ability of DP to inhibit inflammation. Thus, DP inhibits the infiltration of inflammatory cells during wounding [27]. In addition, DP exerts antibacterial effects [28].

Functions of upregulated genes in the Vaseline group were mainly concentrated in the GO:0032502 developmental process direction, including GO:0044767 single-organism developmental process and GO:0048856 anatomical structure development. Results for the Vaseline group are consistent with those of the DP group. Consistency between results of the two groups illustrates that Vaseline does not have major adverse effects on skin wound healing. In addition, through the continuous refinement of the V-collecting GO items, it was found that many of the functions of the last upregulated genes fall in similar directions, such as skin development, including GO:0060429 epithelium development and GO:0043588 skin development. This result indicates the correctness of current model establishment. Downregulated genes mainly functioned in GO:0061061 muscle structure development, which is associated with the development of muscle tissue and cells.

The most enriched pathway for the DP group was rno05322: systemic lupus erythematosus, which involves 30 genes. The most enriched pathway for the Vaseline group was rno05410: hypertrophic cardiomyopathy, which involves 14 genes. The three pathways with the highest degree of gene enrichment in the drug-administered group were the cGMP-PKG signaling pathway, adrenergic signaling in cardiomyocytes, and cAMP signaling pathway. The three pathways with the highest degree of enrichment with downregulated genes were systemic lupus

erythematosus, alcoholism, and ribosome. These results may indicate that the biological activities mediated by these pathways were inhibited. Moreover, cGMP-PKG signaling pathways and cAMP signaling pathways were highly enriched with upregulated genes. These pathways belong to the classical intracellular second messenger regulatory pathway, which is involved in the regulation of various physiological activities. The cGMP-PKG signaling pathway participates in NO-promoted keratinocyte migration. This, in turn, promotes wound healing by transmitting signals [29]. Participation of the cAMP signaling pathway in rat bone tissue formation [30] confirms its role in tissue generation.

Moreover, lncRNAs are functional RNA molecules with lengths of more than 200 nt. They localize in the nucleus or cytoplasm and regulate gene expression on epigenetic, transcriptional, and posttranscriptional levels [31]. They account for 98% of the genome [32] and also play a role in wound healing [33]. They can participate in related inflammatory reactions [34]. Current differential expression analysis identified 601 distinct lncRNAs with potential key roles in wound healing, as illustrated by the results for GO enrichment analysis of their target genes. Cellular processes showed the highest enrichment of lncRNA target genes among all BP-type functional items. The close relationship of numerous functional items in the first 10 items to cell and tissue development is consistent with GO analysis results for mRNA.

Acknowledgements

This work was supported by the Natural Science Foundation of China (820065).

Disclosure of conflict of interest

None.

Address correspondence to: Wenhui Yu, Department of Veterinary Medicine, Northeast Agricultural University, 59 Mucai Street, Xiangfang District, Harbin, China. E-mail: yuwenhui@neau.edu.cn

References

- [1] Kasuya A and Tokura Y. Attempts to accelerate wound healing. *J Dermatol Sci* 2014; 76: 169-72.
- [2] Zeng Q, Xie H, Song H, Nie F, Wang J, Chen D and Wang F. In vivo wound healing activity of

Transcriptomic of wound healing

- abrus cantoniensis extract. *Evid Based Complement Alternat Med* 2016; 2016: 6568528.
- [3] Guo S and DiPietro LA. Factors affecting wound healing. *J Dent Res* 2010; 89: 219-29.
- [4] Laberge A, Arif S and Moulin VJ. Microvesicles: Intercellular messengers in cutaneous wound healing. *J Cell Physiol* 2018; 233: 5550-5563.
- [5] Barrientos S, Stojadinovic O, Golinko MS, Brem H and Tomic-Canic M. Growth factors and cytokines in wound healing. *Wound Repair Regen* 2008; 16: 585-601.
- [6] Burgy O and Konigshoff M. The WNT signaling pathways in wound healing and fibrosis. *Matrix Biology* 2018; 68: 67-80.
- [7] Wu X, Yang LL, Zheng Z, Li ZZ, Shi JH, Li Y, Han SC, Gao JX, Tang CW, Su LL and Hu DH. Src promotes cutaneous wound healing by regulating MMP-2 through the ERK pathway. *Int J Mol Med* 2016; 37: 639-48.
- [8] Zhou T, Yang ZC, Chen YJ, Chen Y, Huang ZW, You B, Peng YZ and Chen J. Estrogen accelerates cutaneous wound healing by promoting proliferation of epidermal keratinocytes via erk/akt signaling pathway. *Cell Physiol Biochem* 2016; 38: 959-68.
- [9] Yan D, Cao Q, Zhao X and Peng D. LncRNA expression profile and bioinformatic analyses of LncRNA-gene network in corneal epithelial wound healing. *Investigative Ophthalmology & Visual Science* 2016; 57.
- [10] Pfaffl MW, Riedmaier-Sprengel I. New surveillance concepts in food safety in meat producing animals: the advantage of high throughput 'omics' technologies-A review. *Asian-Australas J Anim Sci* 2018; 31: 1062-1071.
- [11] Mwenifumbo JC and Marra MA. Cancer genome-sequencing study design. *Nature Reviews Genetics* 2013; 14: 321-332.
- [12] Dang Y, Wang YC and Huang QJ. Microarray and next-generation sequencing to analyse gastric cancer. *Asian Pac J Cancer Prev* 2014; 15: 8033-9.
- [13] Gupta D, Bleakley B and Gupta RK. Dragon's blood: Botany, chemistry and therapeutic uses. *J Ethnopharmacol* 2008; 115: 361-80.
- [14] Xin N, Li YJ, Li X, Wang X, Li Y, Zhang X, Dai RJ, Meng WW, Wang HL, Ma H, Schlaeppi M and Deng YL. Dragon's blood may have radioprotective effects in radiation-induced rat brain injury. *Radiat Res* 2012; 178: 75-85.
- [15] Jiang XW, Qiao L, Liu L, Zhang BQ, Wang XW, Han YW, Yu WH. Dracorhodin perchlorate accelerates cutaneous wound healing in wistar rats. *Evid Based Complement Alternat Med* 2017; 2017: 8950516.
- [16] Namjoyan F, Kiashi F, Moosavi ZB, Saffari F and Makhmalzadeh BS. Efficacy of dragon's blood cream on wound healing: a randomized, double-blind, placebo-controlled clinical trial. *J Tradit Complement Med* 2015; 6: 37-40.
- [17] Li F, Jiang T, Liu W, Hu Q and Yin H. The angiogenic effect of dracorhodin perchlorate on human umbilical vein endothelial cells and its potential mechanism of action. *Mol Med Rep* 2016; 14: 1667-72.
- [18] Zhang P, Li J, Tang X, Zhang J, Liang J and Zeng G. Dracorhodin perchlorate induces apoptosis in primary fibroblasts from human skin hypertrophic scars via participation of caspase-3. *Eur J Pharmacol* 2014; 728: 82-92.
- [19] Chen X, Luo J, Meng L, Pan T, Zhao B, Tang ZG and Dai Y. Dracorhodin perchlorate induces the apoptosis of glioma cells. *Oncol Rep* 2016; 35: 2364-72.
- [20] Rasul A, Ding C, Li X, Khan M, Yi F, Ali M and Ma T. Dracorhodin perchlorate inhibits PI3K/Akt and NF-kappa B activation, up-regulates the expression of p53, and enhances apoptosis. *Apoptosis* 2012; 17: 1104-1119.
- [21] Xia MY, Wang MW, Cui Z, Tashiro SI, Onodera S, Minami M and Ikejima T. Dracorhodin perchlorate induces apoptosis in HL-60 cells. *J Asian Nat Prod Res* 2006; 8: 335-43.
- [22] Zhang G, Sun M, Zhang Y, Hua P, Li X, Cui R and Zhang X. Dracorhodin perchlorate induces G(1)/G(0) phase arrest and mitochondria-mediated apoptosis in SK-MES-1 human lung squamous carcinoma cells. *Oncology Letters* 2015; 10: 240-246.
- [23] Yu JH, Zheng GB, Liu CY, Zhang LY, Gao HM, Zhang YH, Dai CY, Huang L, Meng XY, Zhang WY, Yu XF. Dracorhodin perchlorate induced human breast cancer MCF-7 apoptosis through mitochondrial pathways. *Int J Med Sci* 2013; 10: 1149-56.
- [24] Wei W, Di J, Rasul A, Zhao C, Millimouno FM, Tsuji I, Iqal F, Malhi M, Li X and Li J. Dracorhodin perchlorate induces apoptosis in bladder cancer cells through Bcl-2, Bcl-X-L, survivin down-regulation and caspase-3 activation. *Bangladesh Journal of Pharmacology* 2013; 8: 276-282.
- [25] rapnell C, Roberts A, Goff L, Perteau G, Kim D, Kelley DR, Pimentel H, Salzberg SL, Rinn JL and Pachter L. Differential gene and transcript expression analysis of RNA-seq experiments with TopHat and Cufflinks. *Nat Protoc* 2012; 7: 562-78.
- [26] Yu G, Wang LG, Han Y, He QY. clusterProfiler: an R package for comparing biological themes among gene clusters. *OMICS* 2012; 16: 284-7.
- [27] Yang LF, Liu X, Lv LL, Ma ZM, Feng XC and Ma TH. Dracorhodin perchlorate inhibits biofilm formation and virulence factors of *Candida albicans*. *J Mycol Med* 2018; 28: 36-44.
- [28] Zhan RX, Yang SW, He WF, Wang F, Tan JL, Zhou JY, Yang SS, Yao ZH, Wu J and Luo GX. Nitric oxide enhances keratinocyte cell migration by regulating Rho GTPase via cGMP-PKG signalling. *PLoS One* 2015; 10: e0121551.

Transcriptomic of wound healing

- [29] Shi W, Gao Y, Wang Y, Zhou J, Wei Z, Ma X, Ma H, Xian CJ, Wang J and Chen K. The flavonol glycoside icariin promotes bone formation in growing rats by activating the cAMP signaling pathway in primary cilia of osteoblasts. *J Biol Chem* 2017; 292: 20883-20896.
- [30] Batista PJ and Chang HY. Long noncoding RNAs: cellular address codes in development and disease. *Cell* 2013; 152: 1298-1307.
- [31] Esteller M. Non-coding RNAs in human disease. *Nat Rev Genet* 2011; 12: 861-74.
- [32] Luan A, Hu MS, Leavitt T, Brett EA, Wang KC, Longaker MT and Wan DC. Noncoding RNAs in wound healing: a new and vast frontier. *Adv Wound Care (New Rochelle)* 2018; 7: 19-27.
- [33] Herter EK and Landen NX. Non-coding RNAs: new players in skin wound healing. *Adv Wound Care (New Rochelle)* 2017; 6: 93-107.
- [34] Cui H, Xie N, Tan Z, Banerjee S, Thannickal VJ, Abraham E and Liu G. The human long noncoding RNA Inc-IL7R regulates the inflammatory response. *Eur J Immunol* 2014; 44: 2085-95.